Oceanologia (2019) 61, 265—275

Available online at www.sciencedirect.com

ScienceDirect

journal homepage: www.journals.elsevier.com/oceanologia/

ORIGINAL RESEARCH ARTICLE

The response of cyclonic eddies to typhoons based on satellite remote sensing data for 2001—2014 from the South China Sea

Fangjie Yu [a,b], **Qiongqiong Yang** [a], **Ge Chen** [a,b,*], **Qiuxiang Li** [a]

[a] *College of Information Science and Engineering, Ocean University of China, Qingdao, China*
[b] *Laboratory for Regional Oceanography and Numerical Modeling, Qingdao National Laboratory for Marine Science and Technology, Qingdao, China*

Received 19 August 2018; accepted 26 November 2018
Available online 11 December 2018

KEYWORDS
Tropical cyclones;
Mesoscale eddy;
Eddy kinetic energy

Summary Eddies are known to be affected by typhoons, and in recent years, the general three-dimensional structure, as well as features of the spatial and temporal distributions of eddies have been determined. However, the type of eddy that is most likely to be affected by a typhoon remains unclear. In this paper, quantitative and qualitative methods were used to study the eddies that are most sensitive to upper-ocean tropical cyclones (TCs) from the perspective of eddy characteristics, and the quantitative results showed that not all eddies were enhanced under the influence of typhoons. Enhancement of the eddy amplitude (Amp), radius (Rad), area (A), or eddy kinetic energy (EKE) accounted for 92.3% of the total eddy within the radius of the typhoon. Qualitative analyses showed the following: First, eddies located on different sides of the typhoon tracks were differently affected, as eddies on the left side were more intensely affected by the typhoon than eddies on the right side, and second, eddies with short lifespans or small radii were more susceptible to the TCs.

* Corresponding author at: College of Information Science and Engineering, Ocean University of China, Qingdao, China. Tel.: +86 053266781265.
E-mail address: gechen@ouc.edu.cn (G. Chen).
Peer review under the responsibility of Institute of Oceanology of the Polish Academy of Sciences.

Production and hosting by Elsevier

https://doi.org/10.1016/j.oceano.2018.11.005

1. Introduction

The South China Sea (SCS) is the largest semi-enclosed marginal water body in the Northwest Pacific. Its average depth is 1800 m, and its maximum depth is up to 5400 m. Each year, many TCs pass through the SCS (Liu and Xie, 1999) (Fig. 1), and many studies have shown that their strong winds stir and vertically mix the upper ocean (Guan et al., 2014; Knaff et al., 2013; Price, 1981; Wang et al., 2012), and Mixing of the upper and subsurface water causes the sea surface temperature (SST) to cool (Chiang et al., 2011; Guan et al., 2014; Lin et al., 2017; Liu and Xie, 1999; Potter et al., 2017; Sun et al., 2015).

Due to the influence of seabed topography and kuroshio invasion, many mesoscale eddies occur in the SCS (Chelton et al., 2011b; Du et al., 2016; Wang, 2003; Xiu et al., 2010) that have far-reaching impacts on the mixing of sea water, the transport of deep-sea sediment, and the distributions of marine organisms, energy, heat, and nutrients. As one of the characteristics of oceans, mesoscale eddies can also regulate air–sea interactions (Chelton et al., 2011a; Lin et al., 2005; Patnaik et al., 2014; Shay et al., 2000; Zheng et al., 2010).

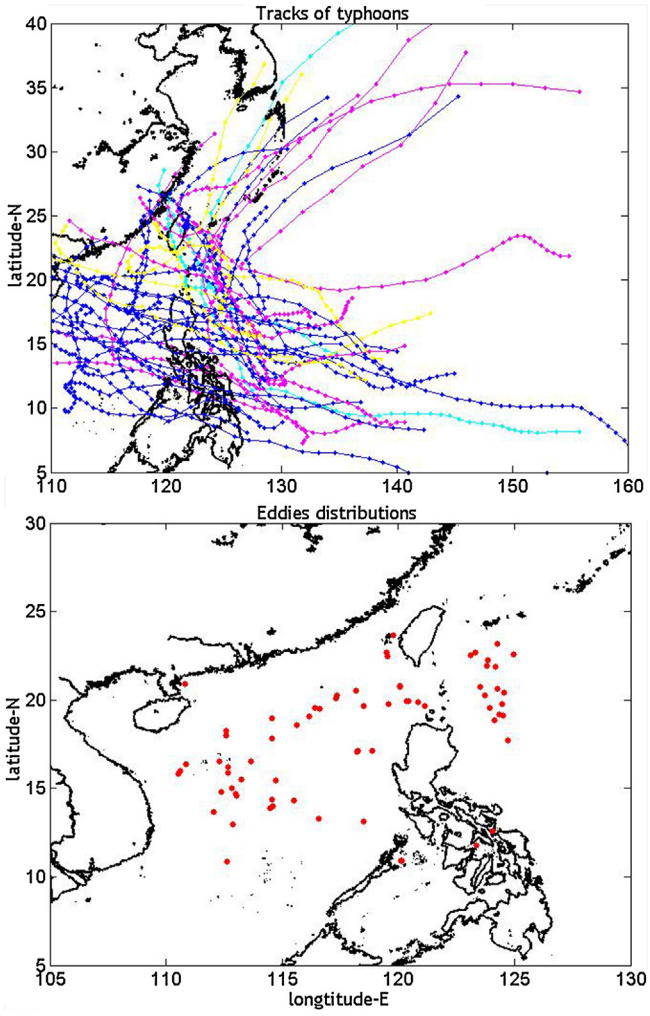

Figure 1 Tracks of typhoons and spatial distributions of eddies.

The interaction between eddies and TCs is an important branch of air–sea interactions, and the study of this interaction improves our understanding of ocean circulation dynamics (Hisaki, 2003; Wang et al., 2009; Zheng et al., 2010). In the past few decades, scholars have suggested that typhoons promote eddy generation. Hu and Kawamura (2004) found that for each case of a looping tropical cyclone, a cyclonic eddy with an obvious sea-level depression appears in the sea area where the cyclone takes a loop form, and a cold core forms with a difference in SST greater than 2°C compared to the surrounding areas (Chen et al., 2012; Chow et al., 2008; Gordon et al., 2017; Hu and Kawamura, 2004; Mahadevan et al., 2008; Zhang et al., 2016). Furthermore, the responses of the cyclonic eddies (CEs) to typhoon forcing in the Western North Pacific Ocean (WNPO) were analyzed using Argo profiles, and the results indicated that the inflow of warm and fresh water, heats and freshens the subsurface in the CEs to compensate for the cooling. Eddies primarily cool at the surface (0–10 m depth) but deep upwelling occurs from the top of the thermocline (200 m in depth) to greater ocean depths shortly after typhoon forcing (Liu et al., 2017). By using satellite and altimeter data to research the response of eddies to typhoons, the eddy core has found to have an obvious sea-level depression after a typhoon, resulting in both mixed layers and SST cooling (Jaimes et al., 2011; Shang et al., 2008); Cyclonic eddies have been found to be enhanced by typhoons, and one noticeable feature was a change in the three-dimensional structure accompanied by reaxisymmetrization and elliptical deformation processes in the horizontal plane (Lu et al., 2016; Wang et al., 2009). Additionally, by comparing the EKE and available gravitational potential energy of COEs before and after typhoons, Sun et al. (2014) found that the energy of a COE can be increased by a slow-moving typhoon, and the EKE can change on order of O (10^{14}–10^{15} J) (Shang et al., 2015; Sun et al., 2014). Finally, among maximum wind speed, typhoon translation speed and the typhoon forcing time (T_f), changes in the geometric and physical parameters of eddies have been found to mostly be related to the T_f, which is determined by typhoon translation speed and size and typhoon intensity (Sun et al., 2014).

In summary, many breakthroughs have occurred in the response of eddies to TCs over the last ten years, but important questions remain unanswered. For example, will the properties of the eddy constrain how it is affected by a typhoon and if so, which kind of eddy responds more strongly? In this paper, the data used for eddy identification and tracking are introduced in Section 2, which is followed by results of the qualitative analysis based on specific eddy and typhoon cases (Section 3). Finally, conclusions are offered that include suggestions for future research (Section 4).

2. Material and methods

2.1. Typhoon data

In this paper, typhoon “best-track data sets” (BTDS) were obtained from the U.S Joint Typhoon Warning Center (JTWC), and each contained typhoon maximum sustained wind (MSW) speeds in knots (i.e., the 1-min mean maximum sustained wind speed at a height of 10 m), the latitude and longitude of

the typhoon center, and the typhoon radius in sea miles. According to the TC classification standard of the JTWC, a TC is defined as a typhoon when its MSW exceeds 63 knots, and as the MSW surpasses 113 knots, a TC is defined as super typhoons. Only TCs in the Northwest Pacific with MSW $\geq$64 knots from 2001 to 2014 were used in this study. The duration of the TCs in the SCS was counted with an accuracy of 0.5 days because the time interval of the BTDS was 6 h (Table 1).

2.2. Satellite data and eddy parameters

Altimeter data from Archiving, Validation, and Interpretation of Satellite Oceanographic Data (AVISO 2014) were used in this study, and they were generated from a combination of data from TOPEX/Poseidon, Jason-1 and Jason-2, and Environmental Satellite. AVISO delayed-time altimeter data from January 1993 to December 2015 are daily, two-satellite merged global seal-level anomalies (SLA) with a spatial resolution 0.25 $\times$ 0.25°. Sea surface temperature (SST) data were acquired from remote sensing systems with a resolution of 25 km. The altimeter data were used to identify, detect and track mesoscale eddies, while SST data were adopted to validate the tracking results. The algorithm used to identify, detect and track mesoscale eddies used in this study was provided by Liu et al. (2016) and Sun et al. (2017). The meridional component, u_g, and the zonal component, v_g, of the geostrophic velocity of the ocean current as well as A and EKE (e.g., Xu et al., 2011) were calculated as follows:

$$A = N\times 0.25\times 0.25\times 111\times 111\times|\cos(lat)|, \quad (1)$$

$$u_g = -\frac{g}{f}\frac{\partial SLA}{\partial y}, \quad v_g = \frac{g}{f}\frac{\partial SLA}{\partial x}, \quad (2)$$

$$EKE = \sum_{i=1}^{n}\frac{1}{2}(u_g^2 + v_g^2)\rho A_i H_i. \quad (3)$$

In those formulas, N is the number of pixel occupied by the eddy, and 0.25 $\times$ 111 transforms the angle into a distance (in kilometer). The variables u_g and v_g are the vertical and horizontal velocity of geostrophic flow, respectively; ρ is a constant value of the density of the seawater equal to 1020 kg m^{-3}; and H_i is the ocean depth. To better illustrate that the eddy is affected by the typhoon this article takes the state of eddy before the typhoon transit as a reference point, the average values of the eddy properties (Amp, Rad, A, EKE) one week after typhoon transit were calculated, and we further calculated the ratio of the eddy attribute values before and after being affected by the typhoon. The reason that ratios were used rather than differences is that an eddy can form at different sizes and because the growth of its properties is also limited. After being affected by a typhoon, the ratio of two eddies with the same property difference may vary greatly; part of the eddy changes significantly during the week after a typhoon and then changes only slightly. Therefore, this article takes the week after the typhoon as the study period and to highlight the impact of typhoons on the upper ocean, the maximum SST and SLA variation are taken at $\pm$2.25° from the eddy center.

Table 1 Information of typhoons.

Typhoon name	Time/day (stay in the SCS)	V_max/knots (Typhoon encountered eddy)	Number of the eddies
PABUK(2001)	2.00	90	2
WUTIP(2001)	5.75	115	3
IMBUDO(2003)	2.25	90	1
MORAKOT(2003)	3.75	120	1
MAEMI(2003)	2.00	65	1
NEPARTAK(2003)	5.75	115	1
CONSON(2004)	2.00	125	1
HAITANG(2005)	4.00	95	1
TALIM(2005)	1.25	115	1
CHANCHU(2006)	6.25	65	4
PRAPIROON(2006)	5.25	115	1
XANGSANE(2006)	4.75	115	3
CIMARON(2006)	10.50	115	3
UTOR(2007)	5.50	75	2
PABUK(2007)	3.00	65	1
SEPAT(2007)	2.00	140	1
PEIPAH(2007)	6.50	75	1
MITAG(2007)	2.50	75	1
NEOGURI(2008)	6.00	100	2
NURI(2008)	3.50	80	2
HAGUPIT(2008)	3.50	100	1
LINFA(2009)	6.75	70	1
MORAKOT(2009)	1.75	80	1
PARMA(2009)	12.00	65	1
FANAPI(2010)	2.25	105	1
MEGI(2010)	5.25	110	4
SONGDA(2011)	1.75	140	2
MUIFA(2011)	5.25	70	1
NESAT(2011)	4.50	75	2
NALGAE(2011)	4.50	65	1
JELAWAT(2012)	2.25	130	1
TINH(2012)	4.25	75	2
BOPHA(2013)	5.00	115	1
SOULIK(2013)	1.25	80	1
NARI(2013)	4.75	80	2
KROSA(2013)	4.75	100	3
HAIYAN(2013)	3.25	95	1
RAMMASUN(2014)	5.00	125	3
MATMO(2014)	1.50	80	1
KALMAEGI(2014)	3.50	70	2

3. Results and discussion

3.1. New eddy generated by Typhoon MEGI (2010)

Typhoon MEGI formed on October 11 and passed through the SCS at 90 knots on October 18, and its direction was from east to west. During its 126-h residency, the intensity of the typhoon increased from 90 knots to 115 knots; MEGI finally left the SCS on October 24 at 30 knots.

The four subgraphs in Fig. 2 illustrate daily SST and SLA on four different days influenced by Typhoon MEGI in the region,

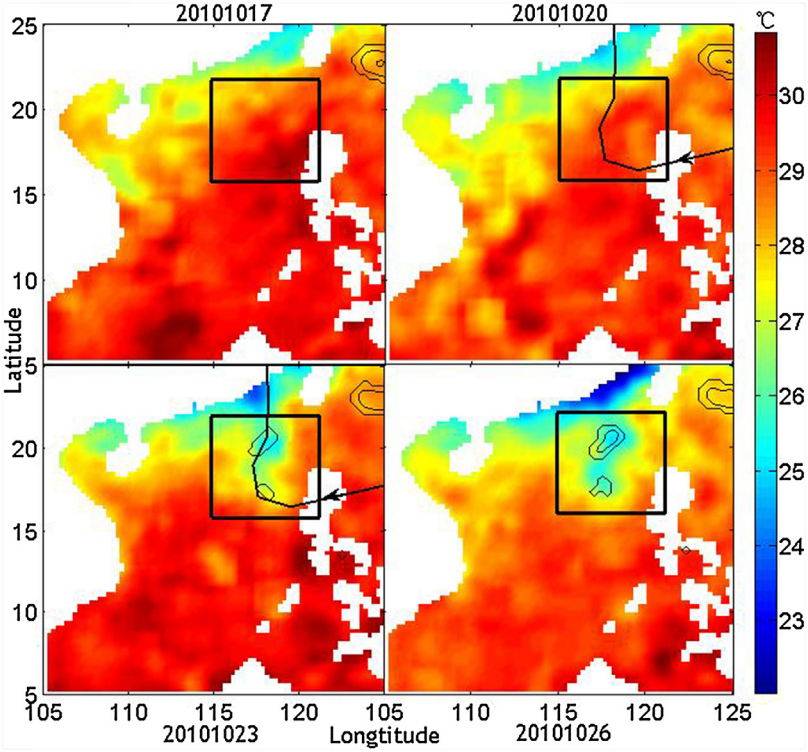

Figure 2 The SST colored, from October 17, 2010 to October 26, 2010. October 17, 2010 was the SST status before the typhoon. October 20, 2010, October 23, 2010, October 26, 2010 were SST status on day 2, day 5 and day 8 after the typhoon, respectively. The curve plots the path of the typhoon, and the arrow marks the direction of the typhoon, the closed loop was the area of SLA < -12 cm (cold eddy zone).

it is obvious that the SST and SLA significantly reduced in the black box area during MEGI period. Before the typhoon's arrival (2010.10.17), the lowest SST of the area of new eddy generation was 27.8°C, and the temperature fell to 27.2°C on the third day (20101020). Then, on the sixth day (2010.10.23) after MEGI, the lowest SST was 25.3°C, which was accompanied by a >12-cm sea-level depression and the appearance of a closed loop. During the 126-h typhoon period, the maximum reduction in SST in the region was 2.53°C, and the maximum reduction of the SLA reached 11.3 cm. In summary, under the influence of the typhoon, a new eddy was generated below the sea on October 23, 2010 (Fig. 2), and this new eddy was well developed and lasted for more than several weeks.

3.2. Typhoon enhanced preexisting eddy

UTOR was a tropical cyclone during the Pacific typhoon season in 2006. The storm formed on December 7, was maintained for 8 days and then dissipated on December 15. The maximum intensity of UTOR during its lifecycle was 100 knots, and UTOR passed the SCS on December 11 with an intensity of 75 knots. Within the range of the radius of UTOR, a mesoscale eddy occurred (recorded as No. 25 eddy in Table 2a, Fig. 4).

Fig. 3 shows the eddy properties of the No. 25 and No. 55 eddy in their whole lifetime. It can be seen from the figure that during the entire life cycle of the eddy, the properties of the eddy are always fluctuating. From the left side of Fig. 3, the SLA, Amp, Rad, Area and EKE of the No. 25 eddy were all significantly changed after affected by UTOR, and the maximum (minimum of the SLA) of each parameter occurred either during or after UTOR. Moreover, compared with other periods, the vital signs of the eddy were relatively stable during the typhoon. The No. 25 eddy was located to the right of the center of UTOR (position of the eddy core relative to the UTOR path) with a radius of 156.92 km and a lifespan of 46 days. After the typhoon passed, the SST in the eddy area decreased by 3.31°C (Fig. 4), and the parameters of No.25 eddy changed. Among them, the SLA decreased by 7.04 cm, and the amplitude, radius, area and EKE increased by1.29 times, 0.92 times, 0.92 times, and 1.15 times respectively, compared to before the typhoon.

Typhoon NARI originated on October 7, 2013 in the Philippines east of the SCS and dissipated on October 16. Its life cycle was 10 days, and its maximum intensity reached 100 knots. When the typhoon passed the SCS, there was an eddy under the typhoon (recorded as the No. 55 eddy in Table 2b, Fig. 5).

The right side of Fig. 3 shows that the SLA, Amp, Rad, Area and EKE of the No. 55 eddy significantly changed after being affected by NARI, and the maximum (minimum of the SLA) of each parameter occurred during or after the typhoon. Moreover, compared with other periods, the vital signs of the eddy were relatively stable during the typhoon. The No. 55 eddy had a lifespan of 42 days and a radius of 52.43 km, and after the typhoon passed, the SST in the eddy area dropped by 2.32°C. The SLA of the eddy core as well as the eddy amplitude, radius, area, and EKE exhibited very significant changes: the SLA decreased by 4.41 cm while the eddy

Table 2a Parameters of 65 eddies.

Eddy	Cold/warm eddy	Location	Lifetime/days	Amp/times	Rad/times	A/times	EKE/times
1	Cold	R	13	1.38	1.15	1.90	5.81
2	Cold	R	13	2.03	1.03	1.19	1.61
3	Cold	R	24	0.79	0.81	0.50	0.33
4	Cold	R	32	1.52	1.15	1.48	1.90
5	Cold	R	24	1.37	1.00	1.59	3.26
6	Cold	L	13	1.51	1.41	2.23	1.51
7	Cold	R	13	0.57	0.92	0.58	3.30
8	Cold	L	13	0.78	0.95	0.75	6.61
9	Cold	R	109	1.12	1.09	0.75	1.59
10	Cold	L	36	1.13	1.10	1.23	2.02
11	Cold	L	14	0.76	0.99	0.68	4.92
12	Cold	L	17	1.07	1.05	1.22	1.19
13	Cold	R	10	2.62	1.57	1.50	4.63
14	Cold	R	32	1.34	1.05	1.11	2.02
15	Cold	R	29	0.36	0.61	0.35	0.14
16	Cold	R	10	0.21	0.43	0.19	0.01
17	Cold	L	15	0.94	0.92	0.93	1.22
18	Cold	L	37	1.35	1.10	2.03	3.77
19	Cold	L	13	2.04	1.60	2.66	8.13
20	Cold	L	13	1.39	1.35	1.81	3.02
21	Cold	R	15	2.13	1.39	0.60	1.63
22	Cold	R	15	2.00	1.48	2.33	13.08
23	Cold	R	15	1.55	1.26	1.66	2.86
24	Cold	R	23	2.35	1.24	1.50	5.09
25	Cold	R	46	1.29	0.92	0.92	1.15
26	Cold	L	12	0.73	1.16	1.20	1.18
27	Cold	L	21	1.54	1.77	2.17	2.91
28	Cold	L	14	2.22	1.27	1.60	1.25
29	Cold	R	18	3.83	1.52	4.87	1.16
30	Cold	R	67	1.16	1.02	0.90	2.14
31	Cold	L	20	0.64	0.78	0.88	0.26
32	Cold	R	27	1.09	0.95	1.09	1.13
33	Cold	L	58	1.18	1.07	0.56	1.19
34	Cold	R	51	1.13	0.97	0.88	1.19
35	Cold	R	27	0.95	0.80	0.65	1.23
36	Cold	L	13	2.62	1.35	1.30	2.39
37	Cold	L	14	1.17	1.00	1.13	1.52
38	Cold	L	45	8.32	3.05	10.25	45.66
39	Cold	R	42	0.75	0.74	0.57	2.24
40	Cold	R	20	0.91	0.70	0.14	0.04
41	Cold	R	42	0.66	0.83	1.01	32.33
42	Cold	R	42	0.64	0.84	1.04	4.86
43	Cold	R	49	0.89	0.87	1.36	2.58
44	Cold	L	27	1.07	0.81	0.26	3.01
45	Cold	R	43	0.78	0.92	0.85	7.73
46	Cold	R	17	0.81	0.91	1.10	0.53
47	Cold	L	24	1.03	1.12	1.26	1.51

amplitude, radius, area, and EKE increased by 1.61 times, 1.06 times, 1.11 times, and 1.99 times, respectively, compared to before the NARI crossed.

With its enhanced amplitude, radius, area, or EKE, the eddy accounted for 92.3% of the total eddies within the radius of the typhoon. The rate of increase in the properties is highly variable among different eddies. In the study, the longest eddy lifespan was 109 days, and the amplitude, radius, area, and EKE of this eddy changed by 1.12, 1.09, 0.75, and 1.59 times, respectively (recorded as the No. 9 eddy in Table 2a). Compared to other eddies that were enhanced by typhoons, this eddy was relatively minimally enhanced. As shown in the next section, this paper takes the perspective of the eddy as a starting point and considers the position of the eddy relative to the typhoon path as well as the lifetime and radius of the eddy to study the reasons for restricted influence of a typhoon.

Table 2b Parameters of 65 eddies.

Eddy	Cold/warm eddy	Location	Lifetime/days	Amp/times	Rad/times	A/times	EKE/times
48	Cold	L	17	0.91	0.99	1.70	137.04
49	Cold	L	21	1.01	0.97	1.11	1.14
50	Cold	R	60	0.92	0.93	1.36	1.44
51	Cold	R	68	1.45	1.08	16.39	26.07
52	Cold	R	21	2.87	1.63	2.39	12.76
53	Cold	L	12	2.37	1.11	2.74	1.79
54	Cold	R	42	1.85	1.13	1.27	3.26
55	Cold	R	42	1.61	1.06	1.11	1.99
56	Cold	L	30	2.40	1.30	2.79	21.27
57	Cold	L	15	1.10	1.20	1.63	6.17
58	Cold	R	51	1.82	1.23	1.12	1.04
59	Cold	R	69	2.14	1.50	2.20	4.37
60	Cold	R	17	1.21	1.11	1.25	1.65
61	Cold	R	17	1.41	1.27	1.80	4.27
62	Cold	R	10	1.78	2.45	7.56	1.20
63	Cold	R	13	3.18	2.28	32.33	4.48
64	Cold	R	13	1.22	1.24	1.33	1.89
65	Cold	R	17	3.06	1.31	1.89	1.55

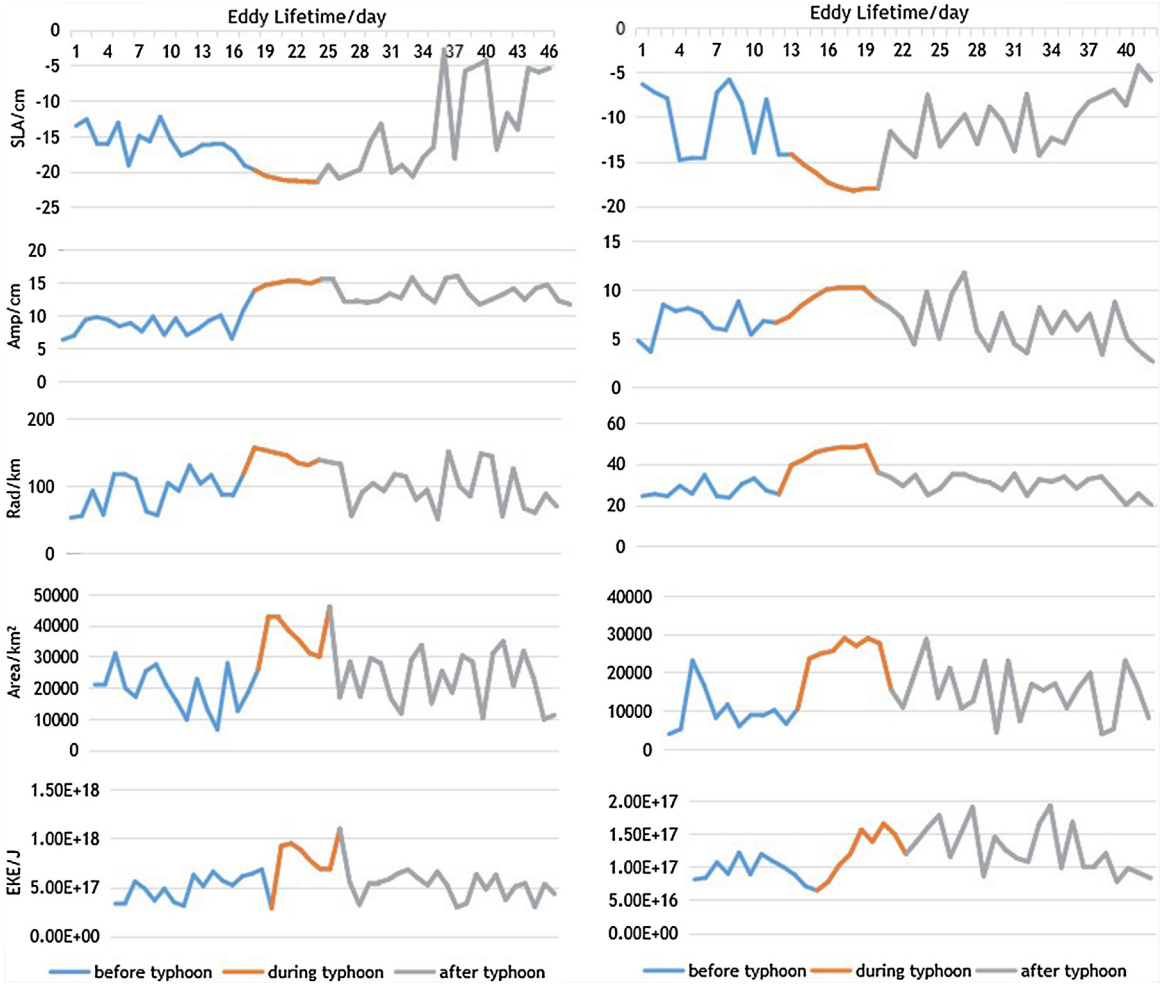

Figure 3 The No. 25 eddy (left) and No. 55 eddy (right) parameters in their whole lifecycle.

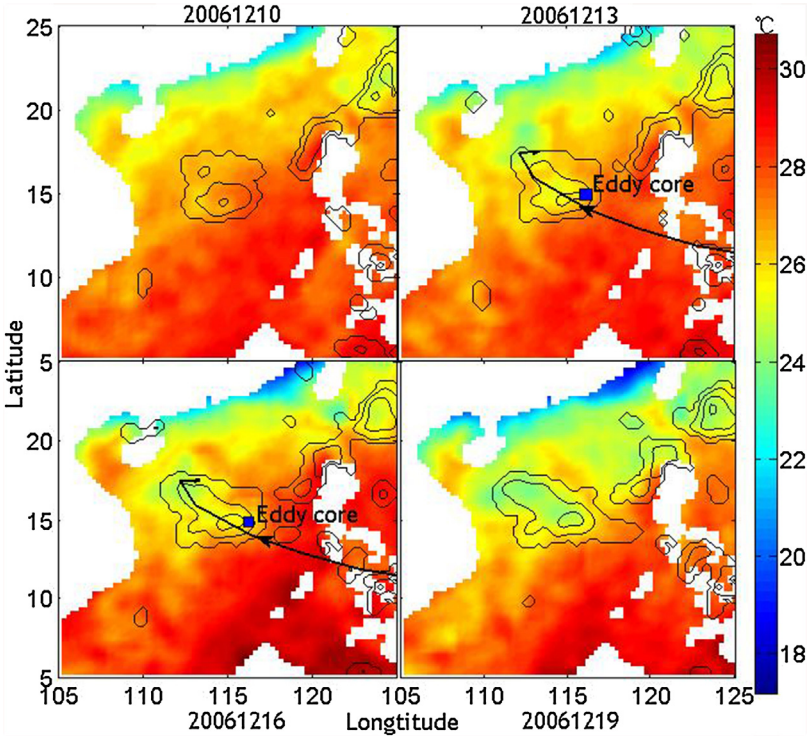

Figure 4 Same as Fig. 2, except for typhoon UTOR, UTOR passed the SCS on December 11, 2006.

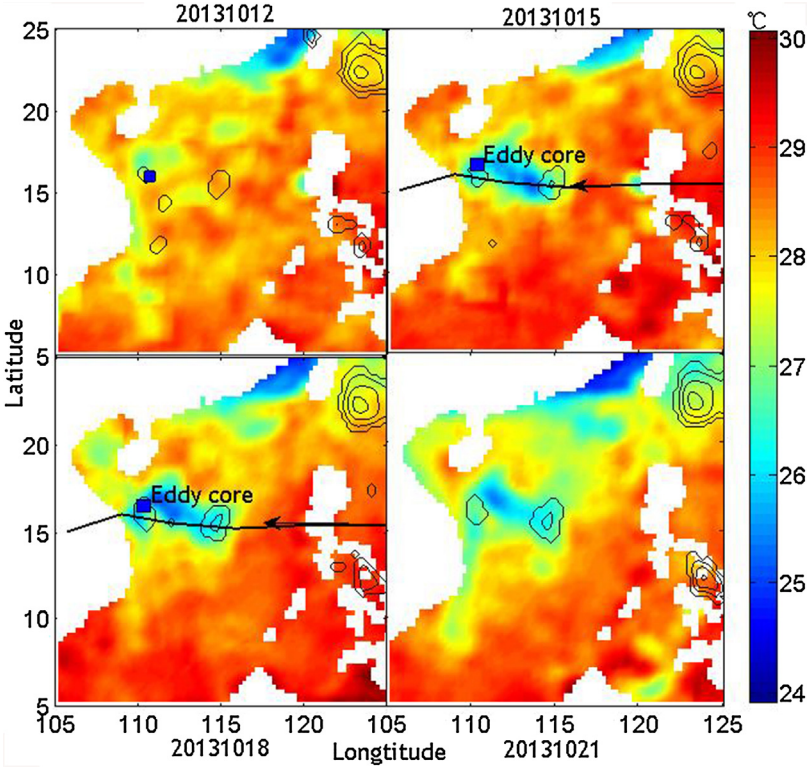

Figure 5 Same as Fig. 2, except for the typhoon NARI, NARI passed the SCS on October 13, 2013.

3.3. Qualitative analysis

The eddy to the left of the typhoon and that to the right were numbered 24 and 41, respectively, accounting for 37% and 63% of the total. Fig. 6 shows that the eddies changed on both sides of the path of the typhoon after the typhoon passed, and seven days after passage, the eddies to the left of the path exhibited greater changes in the SLA, Amp, area and EKE than those to the right. The overall growth trend of the ones on the left of the path was also greater than that for the eddies to the right.

The eddies studied were divided into two groups: those whose radius was larger than the average radius of 75.6 km, referred to as the large eddy group, and those with a smaller-than-average radius km, referred to as the small eddy group. There were 23 eddies in the large eddy group, accounting for 35% of the total, and the small eddy group consisted of 42 eddies, accounting for 65% of the total. Fig. 7 shows the two eddy groups and the changes in their property after the typhoon passed. The result indicates that after being influenced by the typhoon, the eddies with a small radius underwent a more significant increase in their Amp, Rad, area and EKE than those with a large radius. However, after the typhoon passed, the large-eddy Amp and EKE grew only slightly, and their radii and areas decreased. All of these results indicated that a small eddy is more susceptible to a typhoon.

We further divided the eddies into two groups: eddies with lifetimes of 10—20 days were marked as the short-lived group, and eddies with lifetimes longer than 21d were considered as long-lived. There were 32 and 33 short- and long-lived eddies, respectively, each accounting for 50% of the study data. Fig. 8 shows that the values of the two eddy groups increased after being affected by the typhoon, but eddies with a lifespan of 10—20 days exhibited a more intense increase in their Amp, rad, area and EKE than those with lifespan longer than 21 days. The results indicate that short-lived eddies are more susceptible to typhoons than long-lived eddies.

In summary, eddies located on the left of the typhoon path are more intensely affected than eddies on the right. Eddies with the short lifespans and small radii are more susceptible to typhoons.

3.4. Causal relationship

The results of statistical analysis show that the eddy on the left of the typhoon was more intense affected by typhoon than the eddy located on the right side of the typhoon. The difference between the conclusion of this paper and those of others lies in that this paper aims at studying eddies growth rate after being affected by typhoon rather than increment, the latter is concerned with the change in quantity, while this article focuses on indicating the ease or complexity of eddies

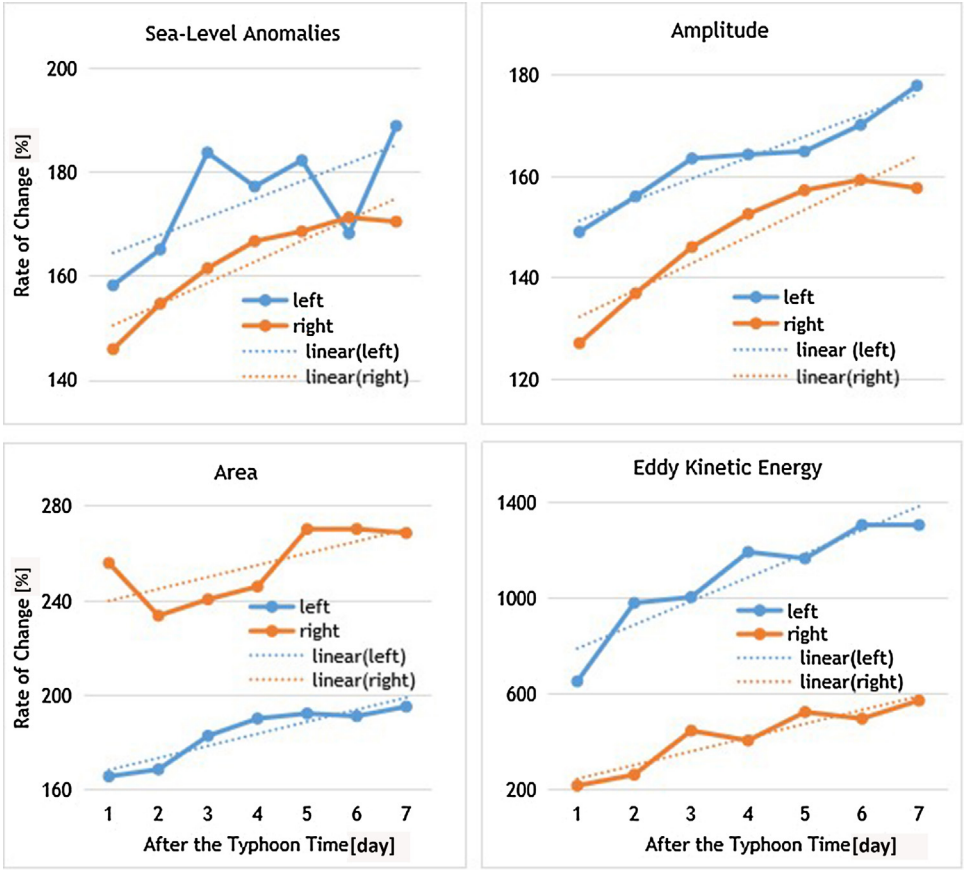

Figure 6 After the typhoon, eddy properties change, on both sides of the typhoon path.

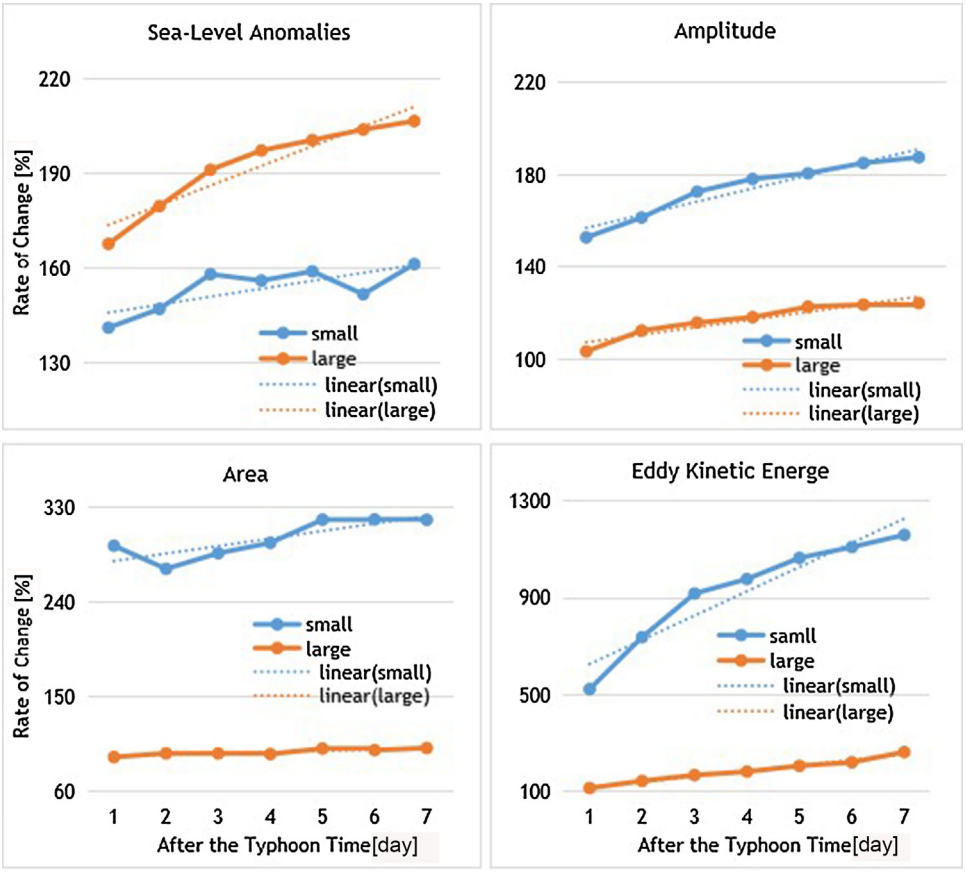

Figure 7 After the typhoon, properties change of large and small eddies.

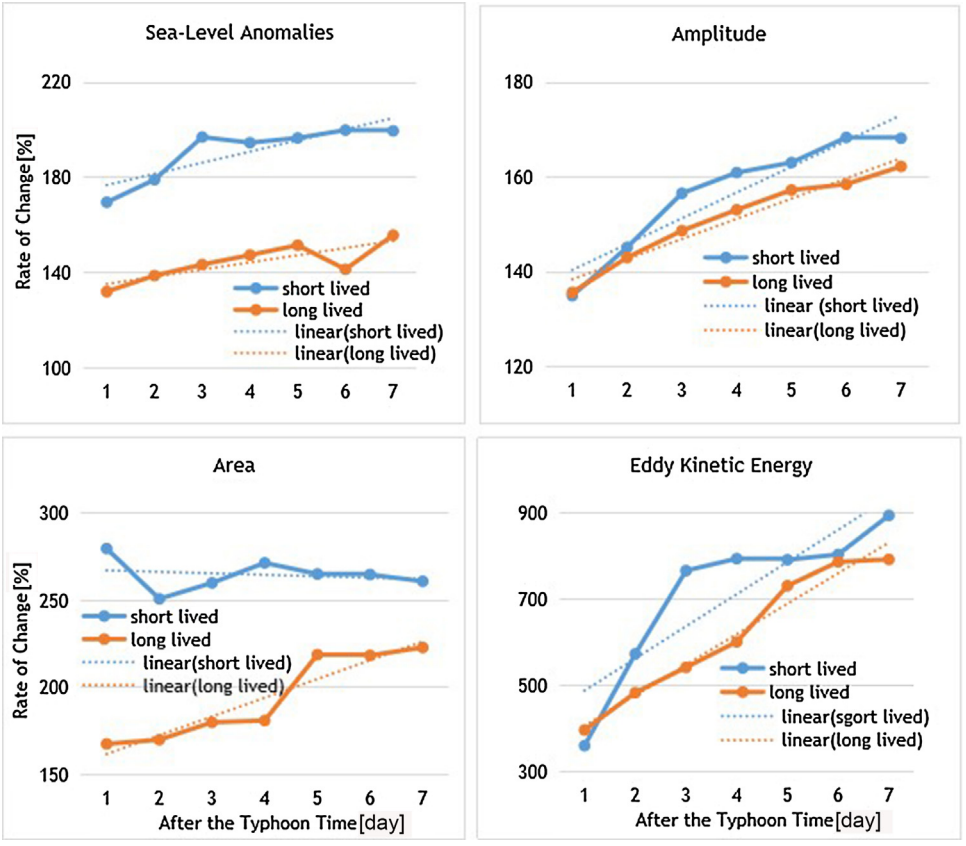

Figure 8 After the typhoon, properties change of short lived eddies and longevity eddies.

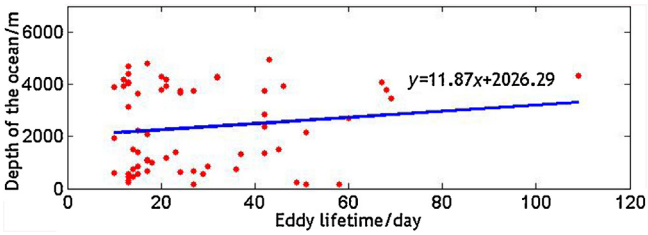

Figure 9 Relationships between eddy lifetime and depth of ocean at the eddy center.

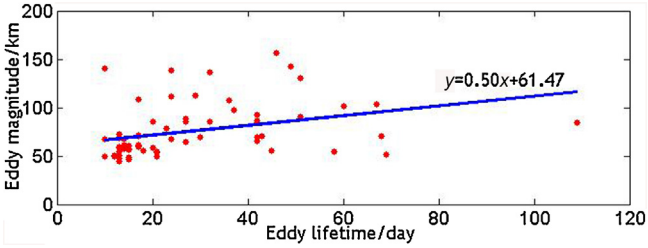

Figure 10 Relationships between eddy lifetime and eddy magnitude.

affected by typhoon. To further study why a short-lived, small-sized eddy was more intensely enhanced by typhoons, the depth of the eddy center and the eddy radius were plotted across the entire eddy life cycle. Fig. 9 shows that long-lived eddies appear more often in deeper sea areas and there appears to be a positive correlation between the lifespan of the eddy and its size. Fig. 10 shows the relationships between the lifespan of the eddy and the depth of the ocean at its center, and it illustrates that short-lived eddies occur more often in shallow seas. This conclusion is consistent with data indicating that strong eddies usually penetrate much deeper into the ocean than weak ones (Xiu et al., 2010).

4. Conclusions

In this study, typhoon and eddy intersection data for 2001 to 2014 for the South China Sea were first generated using typhoon data from JTWC; eddies were then identified and tracked using data from Liu et al. (2016). The data set contained a total of 65 eddies with an average eddy life of 28.03 days and an average radius of 75.6 km. After being affected by a typhoon, not all eddies were enhanced. Typhoon can enhance the eddy, but can't stop the eddy dissipate. When encountered the typhoon in the late stage of its lifecycle, the eddy is hard to be enhanced, it may be explained that the energy dissipated of the eddy itself is greater than that delivered by the typhoon. There are three typical cases demonstrated that typhoons would generate new eddies and enhance preexisting eddies in Section 3. Then, several conclusions were reached through qualitative analysis. First, the Amp, rad and EKE are sharply intensified in eddies located on the left side of the track of the typhoon, and the growth trend is more severe than that of eddies to the right of the track. Second, after being influenced by a typhoon, the Amp, rad, area and EKE of small-sized eddies increase more intensely, and this trend is more prominent compared to eddies with a large magnitude. Third, short-lived eddies are more susceptible to typhoons than long-lived eddies, especially regarding the difference in the eddy radius and area. Finally, the dynamics for the response of mesoscale eddy to the tropical cyclones involves wind stress, and sea surface wind stress was the only way in which the atmosphere can transmit momentum directly to the ocean. This paper was based on the perspective of eddy characteristics, so the wind stress is not introduced in detail, but the specific introduction will be further introduced in the later research on typhoon. Then, it will be possible to expand the study area in the sea, increase the amount of data, and control a single variable to conduct more detailed research about the eddy properties and identify the influence of tropical cyclones alone.

Acknowledgments

The research was supported by following programs: (1) National key research and development program of China (Grant No. 2016YFC1402608, Grant No. 2016YFC1401008); (2) Qingdao National Laboratory for Marine Science and Technology (Grant No. QNLM2016ORP0105); (3) The Fundamental Research Funds for the Central Universities (Grant Nos. 201413064, 201613010).

References

Chelton, D.B., Gaube, P., Schlax, M.G., Early, J.J., Samelson, R.M., 2011a. The influence of nonlinear mesoscale eddies on near-surface oceanic chlorophyll. Science 334 (6054), 328—332, http://dx.doi.org/10.1126/science.1208897.

Chelton, D.B., Schlax, M.G., Samelson, R.M., 2011b. Global observations of nonlinear mesoscale eddies. Prog. Oceanogr. 91 (2), 167—216, http://dx.doi.org/10.1016/j.pocean.2011.01.002.

Chen, G., Gan, J., Xie, Q., Chu, X., Wang, D., Hou, Y., 2012. Eddy heat and salt transports in the South China Sea and their seasonal modulations. J. Geophys. Res.-Oceans. 117 (C5), http://dx.doi.org/10.1029/2011JC007724.

Chiang, T., Wu, C., Oey, L., 2011. Typhoon Kai-Tak: an ocean's perfect storm. J. Phys. Oceanogr. 41 (1), 221—233, http://dx.doi.org/10.1175/2010JPO4518.1.

Chow, C., Hu, J., Centurioni, L.R., Niiler, P.P., 2008. Mesoscale Dongsha Cyclonic Eddy in the northern South China Sea by drifter and satellite observations. J. Geophys. Res. 113 (C4), http://dx.doi.org/10.1029/2007JC004542.

Du, Y., Wu, D., Liang, F., Yi, J., Mo, Y., He, Z., Pei, T., 2016. Major migration corridors of mesoscale ocean eddies in the South China Sea from 1992 to 2012. J. Mar. Syst. 158, 173–181, http://dx.doi.org/10.1016/j.jmarsys.2016.01.013.

Gordon, A.L., Shroyer, E., Murty, V.S.N., 2017. An intrathermocline Eddy and a tropical cyclone in the Bay of Bengal. Sci Rep.-UK 7, 46218, http://dx.doi.org/10.1038/srep46218.

Guan, S., Zhao, W., Huthnance, J., Tian, J., Wang, J., 2014. Observed upper ocean response to typhoon Megi (2010) in the Northern South China Sea. J. Geophys. Res.-Oceans. 119 (5), 3134–3157, http://dx.doi.org/10.1002/2013JC009661.

Hisaki, Y., 2003. Horizontal variability of near-inertial oscillations associated with the passage of a typhoon. J. Geophys. Res. 108 (C12), 12 pp., http://dx.doi.org/10.1029/2002JC001683.

Hu, J.Y., Kawamura, H., 2004. Detection of cyclonic eddy generated by looping tropical cyclone in the northern South China Sea: a case study. Acta Oceanol. Sin. 23 (2), 213–224.

Jaimes, B., Shay, L.K., Halliwell, G.R., 2011. The response of quasigeostrophic oceanic vortices to tropical cyclone forcing. J. Phys. Oceanogr. 41 (10), 1965–1985, http://dx.doi.org/10.1175/JPO-D-11-06.1.

Knaff, J.A., DeMaria, M., Sampson, C.R., Peak, J.E., Cummings, J., Schubert, W.H., 2013. Upper oceanic energy response to tropical cyclone passage. J. Clim. 26 (8), 2631–2650, http://dx.doi.org/10.1175/JCLI-D-12-00038.1.

Lin, I.I., Wu, C.C., Emanuel, K.A., Lee, I.H., Wu, C.R., Pun, I.F., 2005. The interaction of Supertyphoon Maemi (2003) with a warm ocean eddy. Mon. Weather Rev. 133 (9), 2635–2649, http://dx.doi.org/10.1175/MWR3005.1.

Lin, S., Zhang, W., Shang, S., Hong, H., 2017. Ocean response to typhoons in the western North Pacific: composite results from Argo data. Deep-Sea Res. Pt. I 123, 62–74, http://dx.doi.org/10.1016/j.dsr.2017.03.007.

Liu, W.T., Xie, X.S., 1999. Spacebased observations of the seasonal changes of South Asian monsoons and oceanic responses. Geophys. Res. Lett. 26 (10), 1473–1476, http://dx.doi.org/10.1029/1999GL900289.

Liu, Y., Chen, G., Sun, M., Liu, S., Tian, F., 2016. A parallel SLA-based algorithm for global mesoscale Eddy identification. J. Atmos. Ocean. Tech. 33 (12), 2743–2754, http://dx.doi.org/10.1175/JTECH-D-16-0033.1.

Liu, S., Sun, L., Wu, Q., Yang, Y., 2017. The responses of cyclonic and anticyclonic eddies to typhoon forcing: the vertical temperature-salinity structure changes associated with the horizontal convergence/divergence. J. Geophys. Res.-Oceans. 122 (6), 4974–4989, http://dx.doi.org/10.1002/2017JC012814.

Lu, Z., Wang, G., Shang, X., 2016. Response of a preexisting cyclonic ocean Eddy to a Typhoon. J. Phys. Oceanogr. 46 (8), 2403–2410, http://dx.doi.org/10.1175/JPO-D-16-0040.1.

Mahadevan, A., Thomas, L.N., Tandon, A., 2008. Comment on "eddy/wind interactions stimulate extraordinary mid-ocean plankton blooms". Science 320 (5875), 448, http://dx.doi.org/10.1126/science.1152111.

Patnaik, K.V.K.R., Maneesha, K., Sadhuram, Y., Prasad, K.V.S.R., Murty, T.V.R., Brahmananda Rao, V., 2014. East India Coastal Current induced eddies and their interaction with tropical storms over Bay of Bengal. J. Oper. Oceanogr. 7 (1), 58–68, http://dx.doi.org/10.1080/1755876X.2014.11020153.

Potter, H., Drennan, W.M., Graber, H.C., 2017. Upper ocean cooling and air–sea fluxes under typhoons: a case study. J. Geophys. Res.-Oceans. 122 (9), 7237–7252, http://dx.doi.org/10.1002/2017JC012954.

Price, J.F., 1981. Upper ocean response to a hurricane. J. Phys. Oceanogr. 11 (2), 153–175, http://dx.doi.org/10.1175/1520-0485(1981)011<0153:UORTAH>2.0.CO;2.

Shang, S., Li, L., Sun, F., Wu, J., Hu, C., Chen, D., Ning, X., Qiu, Y., Zhang, C., Shang, S., 2008. Changes of temperature and bio-optical properties in the South China Sea in response to Typhoon Lingling, 2001. Geophys. Res. Lett. 35 (10), 6 pp., http://dx.doi.org/10.1029/2008GL033502.

Shang, X., Zhu, H., Chen, G., Xu, C., Yang, Q., 2015. Research on cold core eddy change and phytoplankton bloom induced by typhoons: case studies in the South China Sea. Adv. Meteorol. 2015, 1–19, http://dx.doi.org/10.1155/2015/340432.

Shay, L.K., Goni, G.J., Black, P.G., 2000. Effects of a warm oceanic feature on hurricane opal. Mon. Weather. Rev. 128 (5), 1366–1383, http://dx.doi.org/10.1175/1520-0493(2000)128<1366:EOAWOF>2.0.CO;2.

Sun, L., Li, Y., Yang, Y., Wu, Q., Chen, X., Li, Q., Li, Y., Xian, T., 2014. Effects of super typhoons on cyclonic ocean eddies in the western North Pacific: a satellite data-based evaluation between 2000 and 2008. J. Geophys. Res.-Oceans. 119 (9), 5585–5598, http://dx.doi.org/10.1002/2013JC009575.

Sun, J., Oey, L., Chang, R., Xu, F., Huang, S., 2015. Ocean response to typhoon Nuri (2008) in western Pacific and South China Sea. Ocean Dynam. 65 (5), 735–749, http://dx.doi.org/10.1007/s10236-015-0823-0.

Sun, M., Tian, F., Liu, Y., Chen, G., 2017. An improved automatic algorithm for global eddy tracking using satellite altimeter data. Remote Sens.-Basel. 9 (3), 206, http://dx.doi.org/10.3390/rs9030206.

Wang, G., 2003. Mesoscale eddies in the South China Sea observed with altimeter data. Geophys. Res. Lett. 30 (21), 6 pp., http://dx.doi.org/10.1029/2003GL018532.

Wang, G., Ling, Z., Wang, C., 2009. Influence of tropical cyclones on seasonal ocean circulation in the South China Sea. J. Geophys. Res. 114 (C10), http://dx.doi.org/10.1029/2009JC005302 11 pp.

Wang, H., Wang, D., Liu, G., Wu, H., Li, M., 2012. Seasonal variation of eddy kinetic energy in the South China Sea. Acta Oceanol. Sin. 31 (1), 1–15, http://dx.doi.org/10.1007/s13131-012-0170-7.

Xiu, P., Chai, F., Shi, L., Xue, H., Chao, Y., 2010. A census of eddy activities in the South China Sea during 1993–2007. J. Geophys. Res. 115 (C3), http://dx.doi.org/10.1029/2009JC005657 15 pp.

Xu, C., Shang, X., Huang, R.X., 2011. Estimate of eddy energy generation/dissipation rate in the world ocean from altimetry data. Ocean Dynam. 61 (4), 525–541, http://dx.doi.org/10.1007/s10236-011-0377-8.

Zhang, Z., Tian, J., Qiu, B., Zhao, W., Chang, P., Wu, D., Wan, X., 2016. Observed 3D structure, generation, and dissipation of oceanic mesoscale eddies in the South China Sea. Sci. Rep.-UK 6 (1), 11 pp., http://dx.doi.org/10.1038/srep24349.

Zheng, Z., Ho, C., Zheng, Q., Lo, Y., Kuo, N., Gopalakrishnan, G., 2010. Effects of preexisting cyclonic eddies on upper ocean responses to Category 5 typhoons in the western North Pacific. J. Geophys. Res. 115 (C9), 11 pp., http://dx.doi.org/10.1029/2009JC005562.